Influence of Vortex-Shedding on Interfacial Instabilities in Hybrid Rocket Fuel Liquid Layers

Mae L. Sementilli*, Matthew A. Schulwitz †, Pedram Pakseresht‡, and James Chen§
University at Buffalo, The State University of New York, Buffalo, NY, 14260

With research in hybrid rocket motors becoming of interest due to their controllability and safety, the need has arisen for investigation into how to enhance the performance of these motors to become more comparable to current options. As regression rate is an area of hybrid rocket engine performance that needs to be improved, the introduction of vorticity in the oxidizer flow is a novel method to excite instability in the layer of melted paraffin-based fuel to increase mass entrainment which, in turn, would increase regression rate. In this paper, Volume of Fluid method was explored as a means to simulate the influence of an obstruction in the oxidizer flow, namely the glow plug ignition source used in experimental setups, in shedding vortices to trigger instabilities in the liquid interface. A two-dimensional simulation of cases with and without the glow plug were conducted for a cold-flow case to isolate its hydrodynamic influence on the oxidizer-fuel interactions. Results from these simulations of the slab burner experiment showed significant changes in vorticity generation between cases as well as an increase in mass entrainment by several orders of magnitude. As such, these observations open the door to investigation into the role of vorticity in combustion performance. As more is understood in this area, these insights can aid in prediction of new hybrid motor performance and guide future development.

I. Nomenclature

$\mathbf{F}_\sigma$	=	Volumetric surface tension force
Fr	=	Froude number
$\mathbf{g}$	=	Acceleration due to gravity
L_c	=	Characteristic length
m_{sat}	=	Steady-state mass entrainment
P	=	Pressure
$\dot{r}$	=	Regression rate
Re_L	=	Reynolds number with respect to the characteristic length
t_{sat}	=	Saturation time
U_g	=	Gas velocity
$\mathbf{V}$	=	Velocity field over entire domain
We	=	Weber number
α	=	Phase fraction
κ	=	Interface curvature
ρ	=	Density
ρ_l	=	Density of liquid
ρ_g	=	Density of gas
μ	=	Kinematic viscosity
μ_l	=	Kinematic viscosity of liquid
μ_g	=	Kinematic viscosity of gas
σ	=	Surface tension
τ	=	Viscous stress tensor

*Graduate Student, Department of Mechanical and Aerospace Engineering, 240 Bell Hall Buffalo, NY 14260-4400, and AIAA Student Member.
†Graduate Student, Department of Mechanical and Aerospace Engineering, 240 Bell Hall Buffalo, NY 14260-4400.
‡Postdoctoral Research Associate, Department of Mechanical and Aerospace Engineering, 240 Bell Hall Buffalo, NY 14260-4400.
§Associate Professor, Department of Mechanical and Aerospace Engineering, 240 Bell Hall Buffalo, NY 14260-4400, and AIAA Senior Member.

II. Introduction

HYBRID rocket motors (HRMs) have the potential to become the preferred safe alternative to solid or liquid motors. Currently, there are two main types of rocket engines: liquid and solid. On one hand, liquid motors can be easily throttled but have complex valve systems that can be hazardous to use, in terms of the volatility of the liquid fuels. On the other hand, solid engines are comparatively simple to operate but that simplicity comes at the cost of difficulty in controlling their combustion process. A hybrid rocket engine, which aims to combine the appealing features of both liquid and solid systems, poses a largely unexplored area of modern scientific research.

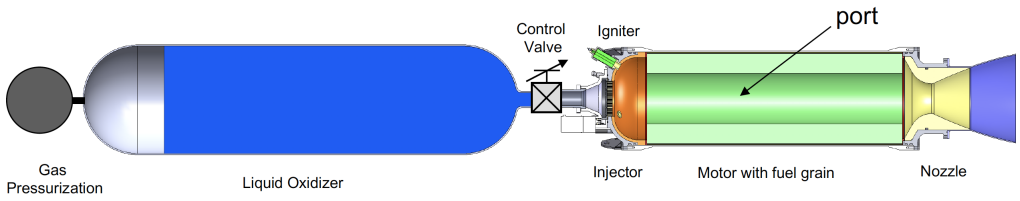

Fig. 1 Typical HRM Layout [1].

As shown in Fig. 1, in a hybrid rocket engine, the liquid or gaseous oxidizer is contained separately from the motor fuel grain and mixing occurs through a controlled injection of oxidizer through the fuel grain housing. This is a much simpler mechanism than that of a liquid rocket motor which is composed of two valve-controlled tanks. An HRM is also more controllable than a solid rocket whose fuel burns freely in air. Since the paraffin-based fuel materials that can be used for hybrid motors are both less volatile and less complex, HRMs may also serve as a more cost-effective alternative to either liquid or solid engines [1]. However, one of the main issues barring the widespread use of hybrid rockets is their overall effectiveness in generating thrust, i.e. insufficient fuel regression rate during the combustion process [1].

The conventional method of increasing regression rate is by increasing the oxidizer mass flux [2], however there are limitations to how much additional entrainment can be obtained by this method. One of the ways explored to combat this is through the use of new fuel materials. It has been found that paraffin wax has a similar regression rate to current cryogenic options [2] and can be further improved with low density polyethylene (LDPE) additives [3].

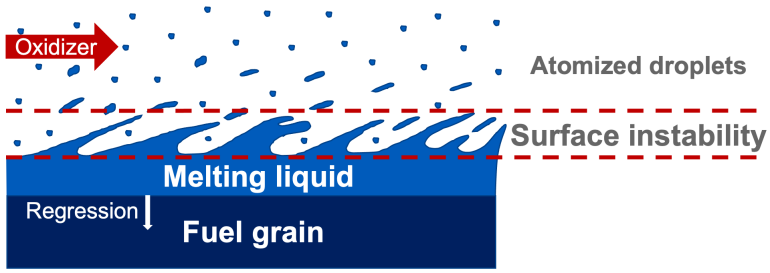

Fig. 2 Schematic of regime layers in an HRM port with formation of fuel droplets.

One of the key mechanisms involved in HRMs is the entrainment of liquid fuel droplets into the oxidizer flow and its direct impact on the combustion process. As shown in Fig. 2, the top layer of solid paraffin fuel melts into a liquid layer during firing. The fuel droplets then become detached from the melting layer due to the fluid interfacial instabilities and are swept into the oxidizer stream. Once they are entrained in the oxidizer, the combustion process occurs and thrust is provided as it expands through the nozzle. An increase in regression rate is directly related to an increase in mass entrainment during the burn [4]. The manual increase of entrainment through the introduction of vorticity into the oxidizer flow, which in turn increases the regression rate of the fuel, is the method which will be explored in this study.

The use of vortices to enhance mixing has been explored in other applications involving spray jet atomization [5], liquid sheet atomization [6], and atomization of gas-liquid flow with combustion [7]. Within the hybrid rocket application, work has been done in comparing theoretical instability models to experimental results by Karabeyoglu and Cantwell [4, 8], primarily comparing how the regression rate is affected by fuel material parameters such as viscosity

and surface tension with oxidizer flow at various Reynolds numbers. Similarly, the influence of the blowing parameter in the oxidizer velocity profile on droplet entrainment was investigated by Bilgin and Cantwell [9]. From these examples, it is plausable that the addition of vorticity would potentially increase entrainment.

To test this, experimental methods are not practical since they are typically expensive and subject to many variables and uncertainties. Additionally, there are limitations to what data can be reasonably collected from the very rapid combustion process. This leaves direct numerical simulation (DNS) as the most cost-effective method to collect information on the mechanisms involved in HRM combustion processes. Specifically, DNS gives the added benefit of allowing prediction of HRM performance under different configurations before experimentally testing a new prototype. However, use of numerical methods to analyze HRMs remains a largely unexplored area. Two of the most widely used techniques for simulating multi-phase flows and tracking the interface between the fluids are Volume of Fluid (VoF) method and Level Set (LS) method. Both methods have their limitations however. In the case of VoF, due to the discontinuous calculations for interface curvature, it can be difficult to effectively capture thin interfaces. On the other hand, although LS can attain a more clear interface description, it does not conserve mass [10]. Taking into consideration this drawback to LS, VoF method has received attention in other general applications such as simulating flows with Kelvin-Helmholtz instabilities in thin films and droplet atomization [11]. In this paper, the VoF technique will also be employed for modeling the interface between two fluid phases in an HRM using the *interFoam* solver available in the open source software OpenFOAM [12].

As a first step in performing a numerical investigation of interfacial instabilities in HRMs, simulations were chosen to replicate the small-scale slab burner experiments conducted by Budzinski et al. [13]. In these experiments, instabilities in the flame as well as additional entrainment of fuel droplets into the oxidizer flow were observed directly downstream of the glow plug, a mechanism used to trigger the combustion process. The simulations conducted in this study were chosen to replicate this behavior and discover the root cause of this instability. It was postulated that this may be the result of vortex shedding from the glow plug exciting Kelvin Helmholtz instability as it perturbs the surface of the liquid fuel, thus causing additional mass entrainment. Looking into this question leads further to the more general characterization of how atomization takes place in an HRM and what can dynamically influence it. The results of this study into instability generation can result in better understanding of whether the data collected in the experiment may have been contaminated by the presence of the glow plug.

The subsequent sections of the paper are arranged as follows: Section III which describes the employed mathematical formulation and validation cases, Section IV which explains the results of the slab burner simulations, and Section V which concludes the paper with final remarks and summary of the work.

III. Methodology

A Volume of Fluid method was used to simulate the flow field of two immiscible, incompressible fluids by solving the governing equations with both fluids as a single flow field, using weighted values for the density, viscosity and other properties [12]. In this approach, the governing equations include continuity and momentum equations in addition to a transport equation for the liquid phase fraction, α, as expressed in Eqs. (1)-(3) [12].

$$\nabla \cdot \mathbf{V} = 0 \tag{1}$$

$$\frac{\partial(\rho\mathbf{V})}{\partial t} + \nabla \cdot (\rho\mathbf{V}\mathbf{V}) = -\nabla P + \nabla \cdot \tau + \rho\mathbf{g} + \mathbf{F}_\sigma \tag{2}$$

$$\frac{\partial \alpha}{\partial t} + \nabla \cdot (\alpha\mathbf{V}) = 0 \tag{3}$$

where $\mathbf{V}$ represents the velocity field of the effective fluid throughout the entire domain, $\mathbf{V} = \alpha\mathbf{V}_l + (1-\alpha)\mathbf{V}_g$ [12]. For any given computational cell, the phase fraction can range from 0 to 1, corresponding to all oxidizer or all fuel, respectively. Accordingly, the density and viscosity of each cell are calculated using the known α as,

$$\rho = \rho_l\alpha + \rho_g(1-\alpha) \tag{4}$$

$$\mu = \mu_l\alpha + \mu_g(1-\alpha) \tag{5}$$

To model the surface tension on the interface layer, $\mathbf{F}_\sigma$, the Continuum Surface Force (CSF) model is used, in which an estimation of the interface curvature is made for each computational cell [14]. The employed expression for CSF is expressed as,

$$\mathbf{F}_\sigma = \sigma\kappa(\alpha)\boldsymbol{\nabla}\alpha \tag{6}$$

where,

$$\kappa(\alpha) = -\nabla \cdot \left(\frac{\nabla\alpha}{|\nabla\alpha|}\right) \tag{7}$$

is the interface curvature. This model is prevalent in VoF implementation, however, it is known that this estimation of surface curvature creates spurious velocity values [15]. A remedy for such a problem would be coupling VoF method with a Level Set method for the interface reconstruction that could result in better prediction for sharper gradients at the interface. This requires replacing α with the level set field which in turn introduces a correction for surface tension, viscosity, and density values [10, 16]. Such a coupling technique can reduce the spurious velocities mentioned above [17], however, this is not the focus of the current study.

IV. Results

In this section, the predictive capability of the employed VoF method for studying instabilities was first assessed. Then, the methodology was utilized for investigating the interfacial instabilities of a slab burner case, resembling a subsection an HRM.

A. Validation Study

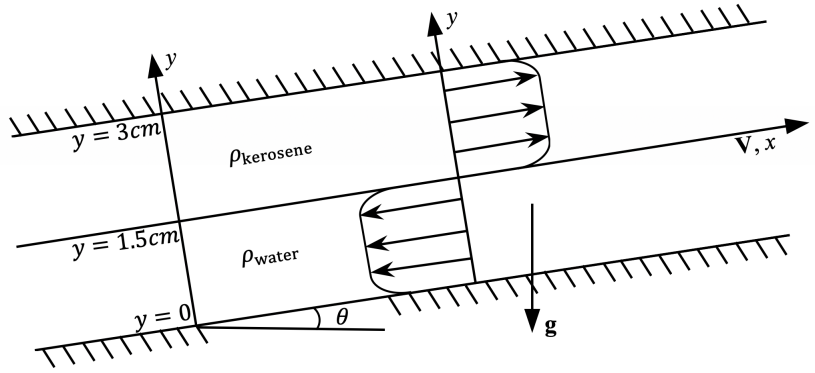

Fig. 3 Schematic of the tilted tank used for the validation study.

In order to ensure that any instability growth can be accurately captured using VoF, a validation case was performed. Experimental work by Thorpe [18] on a gravity driven flow was simulated using VoF. In the experiment a rectangular tank, with dimensions of $183 \times 3 \times 10\ cm^3$ and filled fully with equal quantities of kerosene and water, was tilted at an angle of $\theta = 4.129°$ from horizontal, as shown in Fig. 3. The difference in the density of the fluids creates a wavelike instability growth at the central region of the interface between the fluids. The denser fluid, water, flows to the left toward the lower end of the tank while the lighter fluid, kerosene, rises to the higher end on the right.

Table 1 Grid study

Case	Grid Resolution, *	Onset Time, *s*
Thorpe [18]	–	2.12
Coarse	10	2.70
Fine	20	2.16

* Number of grids per *cm*

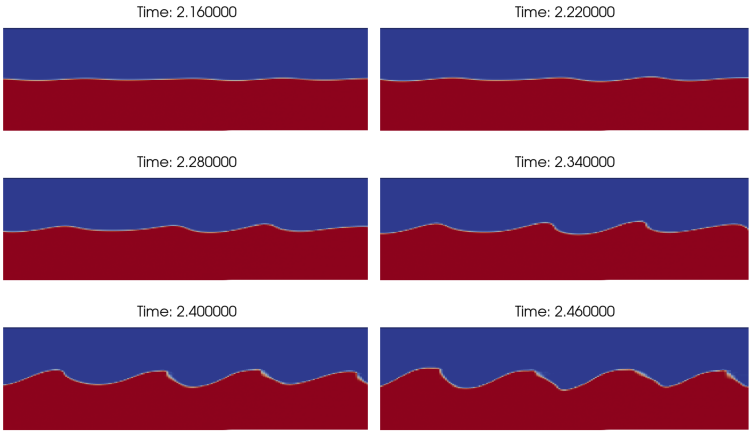

Fig. 4 Qualitative instabilities of validation case simulation. Time is in seconds.

A fine and coarse mesh were evaluated for this simulation, with the fine mesh having twice the number of cells per unit length. As shown in Table 1, the onset of instability observed in the experiment started at $2.12s$, defined as the time when variations in the interface exceed $1mm$. With finer grid resolution, the time of onset of instability differed by 1.8% from the experiments while the coarse mesh differed by 27.4%. The maximum wave height was essentially the same for all three cases, with the growth in wave height happening comparatively slower for the coarse grid resolution. The fine grid resolution, the results of which are shown in Fig. 4, was found to be sufficient for the presented simulations with results being independent of the grid for finer resolutions.

B. Slab Burner Simulation

The 2-D simulations were designed to replicate the small-scale slab burner experiment as described in Budzinski et al. [13]. Additionally, by choosing to numerically recreate this experiment, it is also possible to examine the potential of exciting interfacial instabilities between two fluids through vortex shedding from the glow plug ignition source used in the experiment.

Fig. 5 The small-scale slab burner experimental set up.

In the slab burner experiment, a fully developed gaseous oxidizer flows into a combustion chamber which contains a small slab of paraffin wax fuel. A glow plug was used to ignite the slab of wax in a way that is consistent between different experimental test runs. Fig. 5 shows the layout of the experimental combustion chamber and specifically identifies the oxidizer inlet, glow plug, and wax fuel slab [19, 20]. This glow plug is a heated piece of metal that is mechanically lowered from the top of the chamber and makes contact with the front slope of the wax slab to cause ignition. After ignition, the glow plug is then raised back out of the chamber while the wax fuel is allowed to fully combust [13]. This process can be viewed through the transparent walls of the chamber for analysis.

As a result of using the glow plug in the experiment, it was conjectured that its presence might disturb the flow of the oxidizer over the liquefying top layer of wax fuel such that an instability might form at their interface. To assess such an observation, two simulations focusing on the fluid dynamics within the chamber are performed for two cases: either with or without the presence of the glow plug. These cases are designed to resemble the 2-D domain illustrated in Fig. 5.

Consistent with the experiment, the gaseous oxidizer enters the domain from an inlet at the left wall and exits through an outlet at the right wall. The indentation along the top wall (see Fig. 5b) represents the geometry of the glow plug while the indentation along the bottom wall in both domains represents the wax fuel slab. To represent the fuel regression process, an inlet of liquid wax is placed along the bottom wall. This inlet begins at the leading edge of the wax fuel slab and ends halfway down its length. The liquid wax enters with a uniform constant velocity profile and is also allowed to exit the domain through the outlet at the right. It should be noted that the size and shape of the indentation along the bottom wall representative of the wax fuel slab does not change during the simulation, contrary to the actual physical process of melting wax. This is done as a simple technique to isolate the effects of the glow plug. The goal of which is to observe the interfacial instabilities at the fluid interface between the gaseous oxidizer and liquid wax caused by the vortex shedding from the glow plug while avoiding unnecessary complexity in the simulation.

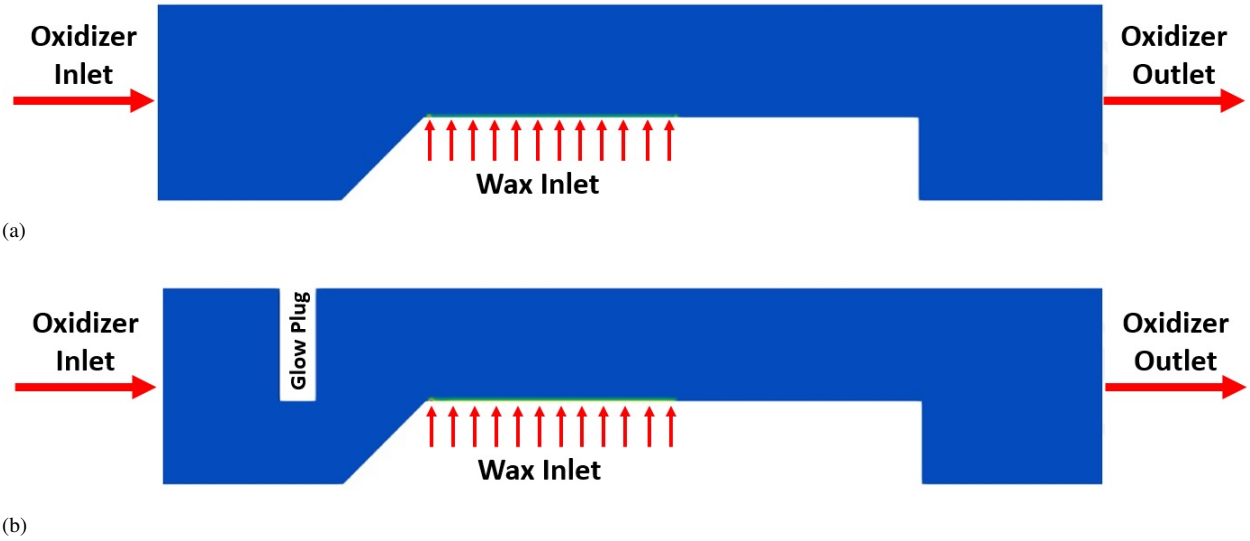

Fig. 6 The 2-D slab burner simulation domain (a) without glow plug, (b) with glow plug.

The overall dimension of the simulated domains are consistent with the size of the experimental setup described by Budzinski et al. [13]. In the 2-D symmetry plane, the total length and height are 14 cm and 2.69 cm, respectively. The total height of the domain also serves as the characteristic length, L_c used for the parameter calculations of the simulation. The glow plug is 0.5 cm wide by 1.55 cm tall and is positioned such that its left side is 2.115 cm from the domain inlet. The wax slab is 8 cm long by 1.14 cm tall and the angle at the leading edge is 45° with respect to the bottom of the domain. The lower front tip of the wax slab is positioned 3 cm from the domain inlet. This coincides with the outlet length of 3 cm from the trailing edge the wax slab. The oxidizer inlet has a parabolic velocity profile with a maximum velocity, U_g, of 10 m/s. The wax inlet velocity has a uniform magnitude of 1 mm/s upwards into the domain. The value of $\dot{r} = 1\ mm/s$ was chosen as it conforms to the experimentally observed wax regression rate as a consequence of the chosen oxidizer inlet velocity per Budzinski et al. [13]. The density ratio for the two fluid phases, liquid wax and gaseous oxidizer, ρ_l/ρ_g is 750. The viscosity ratio for these two fluids, ν_l/ν_g is 0.476. The Reynolds Number, defined as $Re = \rho_g U_g L_c/\nu$, is approximately 17000; the Froude Number, defined $Fr = U_g^2 L_c/g$, is approximately 400; and the Weber number characterizing the ratio of the inertial and surface tension effects, defined as $We = \rho_g U_g^2 L_c/\sigma$, is approximately 72. A list of the boundary conditions used in the simulations can be found below in Table 2.

C. Simulation Results

The vorticity contours shown in Fig. 7a and 7b are the results of the flow taken at 0.1 s. This time was chosen as it is sufficient for the flow field to become fully developed.

Table 2 Simulation Boundary Conditions

Boundary	Velocity	Pressure
Inlet	Fixed	Zero Gradient
Wax Inlet	Fixed	Zero Gradient
Outlet	Zero Gradient	Atmosphere
Top Wall	No Slip	Fixed Gradient
Bottom Wall	No Slip	Fixed Gradient

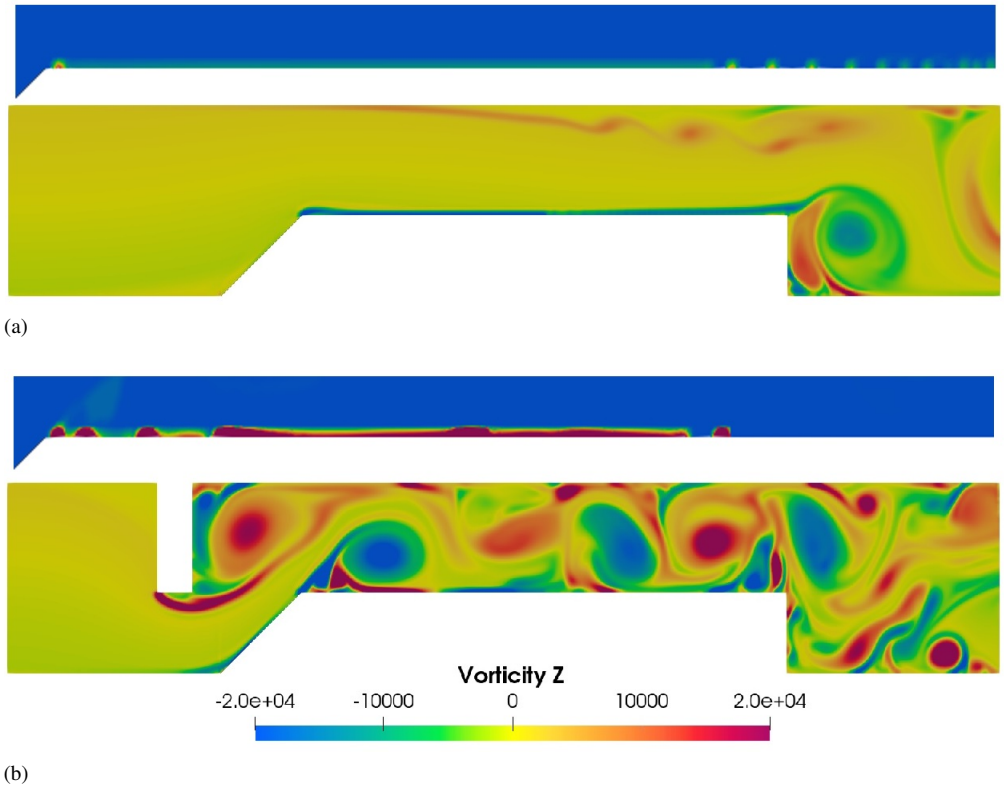

Fig. 7 Vorticity contours for the simulated small-scale slab burner experiment at $0.1\ s$ **(a) without glow plug, (b) with glow plug. Above each vorticity contour is a zoomed-in view of the corresponding oxidizer-wax interface.**

As illustrated in Fig. 7a, in the case without the influence of the glow plug, the vorticity of the flow was mostly uniform accross the entire length of the oxidizer-wax interface. This was starkly contrasted by the vorticity contour in Fig. 7b, which shows a large variation in the vorticity for the case where the glow plug is present in the domain. It is also evident qualitatively that a Von Karman street is developing behind the glow plug and impacting the fuel surface. Additionally, compared to the smooth surface in the top cutout in Fig. 7a, the formation of an instability at the oxidizer-wax interface can clearly be seen in the zoomed-in portion of Fig. 7b.

To further explore the mass entrainment, cases with three different regression rates ($\dot{r}_{norm}$ = 1, 2, and 10) were conducted, with $\dot{r}_{norm}$ = 1 corresponding with a value similar to experimental rates, and having the same oxidizer flow rate (U_g= 10 m/s) for all cases. To quantify mass entrainment, the mass of liquid fuel was summed in the red boxed region specified in Fig. 8, whose area is 7.06 cm^2, at every time step of the simulation. The results were then smoothed using a Gaussian filter to show the general trend.

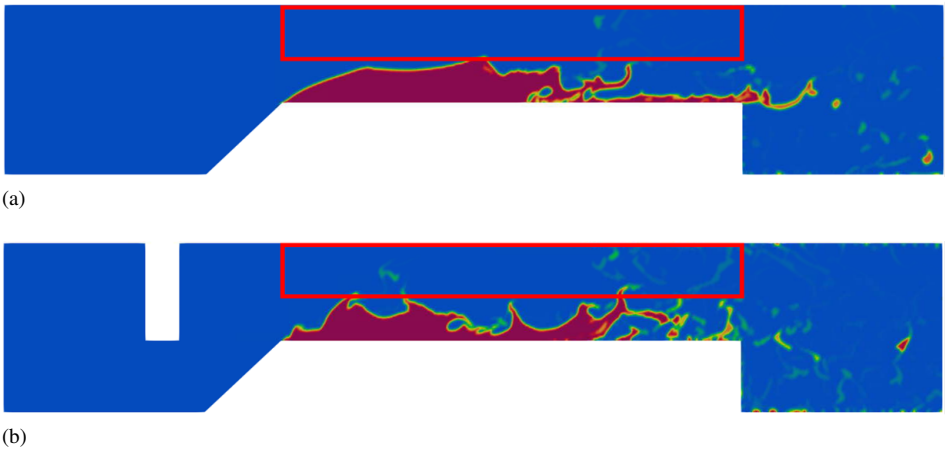

Fig. 8 Region for mass entrainment calculation for $\dot{r}_{norm} = 10$ (a) without (b) with glow plug.

Table 3 Comparison of mass entrainment and saturation time.

$\dot{r}_{norm}$	m_{sat} w/ glow plug	m_{sat} w/o glow plug	t_{sat} w/ glow plug	t_{sat} w/o glow plug
1	3.144×10^{-3}	2.041×10^{-26}	0.353	0.805
2	6.490×10^{-3}	2.606×10^{-5}	0.238	0.349
10	3.731×10^{-2}	2.106×10^{-2}	0.075	0.042

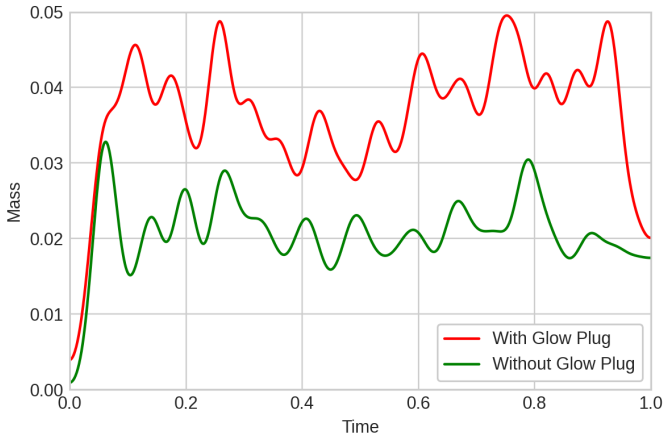

Fig. 9 Comparison of mass entrainment over t =1 s for $\dot{r}_{norm}$=10.

Figure 9 compares the difference in the steady state value of mass in the entrainment region for cases with and without the glow plug, showing that the case including the glow plug has a higher mass entrainment. According to predictions made in theoretical models by Karabeyoglu [8], the oxidizer flux used in these simulations was lower than the cut off necessary for mass entrainment. As shown in Table 3, observations of the mass entrainment without the glow plug had little to no entrainment as expected, making it clear that vorticity from the glow plug was the cause of entrainment observed. It is also clear that for smaller regression rates the entrainment is multiple magnitudes greater when the glow plug is present, with the lowest regression rate case having essentially no mass entrained without the glow plug and substantial entrainment with the glow plug. This confirms the hypothesis that the vorticity generated by the glow plug has a positive influence on mass entrainment. Also from knowledge of the heat transfer in experiments

[8], this increased mass entrainment will result in a thinner liquid layer, thus further increasing the regression rate. This positive feedback would theoretically lead to improved engine performance. It can also be noted that the rate of increasing mass in the region for the transient portion of the test is the same for both cases in Fig. 9.

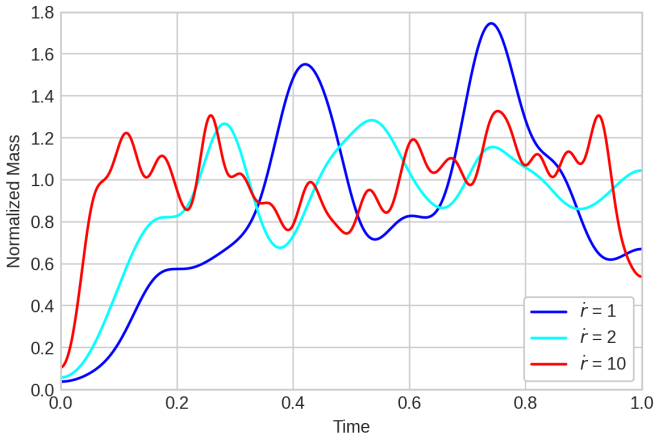

Fig. 10 Saturation time comparison for $\dot{r}$ =1, 2, 10.

In Fig. 10 the mass was normalized by m_{sat} for each case to compare the time taken to reach the saturation value. This plot shows decreasing t_{sat} with a corresponding increase in regression rate. Table 3 shows that the time to saturation for the cases without the glow plug echo this trend, but are comparatively longer in time to the cases with the glow plug at low regression rate. Since the regression rates observed in Budzinski et al. [13] are similar to the lowest regression rate of $\dot{r}_{norm} = 1$, the potential increase in mass entrainment is considerable. With this mass entrainment being comparable to that of higher regression rates, the use of vortex shedding is a promising method for increasing combustion efficiency.

V. Conclusion

Hybrid Rocket Motors provide an exciting new avenue in the future of rocket design. However, while there are potentially substantial safety, control, and environmental benefits, there remains the need to improve the understanding of the physical processes which govern HRM combustion. By using modern computational tools and techniques, VoF simulations can begin to be developed which aim to better describe complex HRM systems. As methods are improved, these simulations will be able to make predictions on the effectiveness of different HRM configurations faster and more easily than by only using experimental methods.

The excitation of interfacial instabilities in the liquid fuel interface of the HRM is a promising area of research to increase regression rate. By creating 2-D models of a small-scale slab burner experiment, characteristics of the interaction between a gaseous oxidizer and melting liquid wax layer can be quantified. Simulating the glow plug component of the experimental setup showed the excitation of the oxidizer-wax interface through vorticies shed from the upstream object. These excitations are the source of notable effects in the downstream flow field quantities which caused the oxidizer to interact with the liquid wax top layer and led to increased interfacial instabilities which can potentially increase regression rate.

In addition, the mass entrainment is clearly improved by the vorticity generated by the glow plug upstream of the fuel grain. This has significance because the oxidizer mass flow rate was held constant for all of these test cases, showing an ablity to increase mass entrainment (and subsequently increase the surface area for improved combustion efficiency) without increasing oxidizer consumption. This difference is most pronounced at low regression rate, which is more similar to experimental observations, where mass entrainment is essentially zero without the glow plug but on the same order of magnitude as higher regression rates when the glow plug is present. This use of vortex-shedding could potentially open another path to explore for increasing the efficiency of HRM performance. These simulations also open the door to understanding the multi-physics present in HRMs which could not be readily observed and have not previously been studied.

Acknowledgments

This research is funded by the United States Department of Energy's (DoE) National Nuclear Security Administration (NNSA) under the Predictive Science Academic Alliance Program III (PSAAP III) at the University at Buffalo, under contract number DE-NA0003961. Support provided by the Center for Computational Research at The University at Buffalo [21]. M. L. S., M. A. S., and J. C. thank Dr. Marianne Francois of Los Alamos National Laboratory (LANL) for her technical consultation and guidance.

References

[1] Cantwell, B. J., "AA283 Aircraft and Rocket Propulsion: Chapter 11, Hybrid Rockets," , 2007. Stanford University course notes.

[2] Karabeyoglu, M. A., Cantwell, B. J., and Altman, D., "Development and testing of paraffin-based hybrid rocket fuels," *37th Annual Joint Propulsion Conference and Exhibit*, AIAA, Salt Lake City, Utah, 2001, pp. 1–24.

[3] Kim, S., Lee, J., Moon, H., Sung, H., and Kim, J., "Effect of paraffin-LDPE blended fuel in hybrid ricket motor," *46th Annual Joint Propulsion Conference and Exhibit*, AIAA, Nashville, TN, 2010, pp. 1–16.

[4] Karabeyoglu, M. A., and Cantwell, B. J., "Combustion of liquefying hybrid propellants: Part 2, Stability of liquid films," *Journal of Propulsion and Power*, Vol. 18, No. 3, 2002, pp. 621–630.

[5] Depuru-Mohan, N. K., Greenblatt, D., Nayeri, C. N., Pashereit, C. O., and Panchapakesan, N. R., "Vortex-enhanced mixing through active and passive flow control methods," *Experiments in Fluids*, Vol. 56, No. 51, 2015, pp. 1–16.

[6] Zandian, A., Sirignano, W. A., and Hussain, F., "Understanding liquid-jet atomization cascades via vortex dynamics," *Journal of Fluid Mechanics*, Vol. 843, 2018, pp. 293–354.

[7] Vera, M., and Linan, A., "On the interaction of vortices with mixing layers," *Physics of Fluids*, Vol. 16, No. 7, 2004, pp. 2237–2254.

[8] Karabeyoglu, M. A., Altman, D., and Cantwell, B. J., "Combustion of liquefying hybrid propellants: Part 1, General theory," *Journal of Propulsion and Power*, Vol. 18, No. 3, 2002, pp. 610–620.

[9] Bilgin, E., and Cantwell, B. J., "Combustion of liquid hybrid propellants: long wave instabilities of sheared liquid films subject to blowing," *AIAA Propulsion and Energy 2020 Forum*, AIAA, Virtual, 2020, pp. 1–10.

[10] Nichita, B. A., Zun, I., and Thome, J. R., "A level set method coupled with a volume of fluid method for modeling of gas-liquid interface in bubbly flow," *Journal of Fluids Engineering*, Vol. 132, No. 8, 2010, pp. 1–18.

[11] Kazimardanov, M. G., Mingalev, S. V., Lubimova, T. P., and Gomzikov, L. Y., "Simulation of primary film atomization due to Kelvin-Helmholtz instability," *Journal of Applied Mechanics and Technical Physics*, Vol. 59, No. 7, 2018, pp. 1251–1260.

[12] Damian, S. M., "Description and utilization of interFoam multiphase solver," *International Center for Computational Methods in Engineering*, 2012, pp. 1–64.

[13] Budzinski, K., Aphale, S. A., Katz-Ismael, E., Surina, G., and DesJardin, P., "Radiation heat transfer in ablating boundary layer combustion theory used for hybrid rocket motor analysis," *Combustion and Flame*, Vol. 217, 2020, pp. 248–261.

[14] Brackbill, J. U., Kothe, D. B., and Zemach, C., "A Continuum Method for Modeling Surface Tension," *Journal of Computational Physics*, Vol. 100, 1992, pp. 335–354.

[15] Francois, M. M., Cummins, S. J., Dendy, E. D., Kothe, D. B., Sicilian, J. M., and Williams, M. W., "A balanced-force algorithm for continuous and sharp interfacial surface tension models within a volume tracking framework," *Journal of Computational Physics*, Vol. 213, 2006, pp. 141–173.

[16] Albadawi, A., Donoghue, D. B., Robinson, A. J., Murray, D. B., and Delaure, Y. M. C., "Influence of surface tension implementation in Volume of Fluid and coupled Volume of Fluid with Level Set methods for bubble growth and detachment," *International Journal of Multiphase Flow*, Vol. 53, 2013, pp. 11–28.

[17] Cao, Z., Dongliang, S., Wei, J., Yu, B., and Li, J., "A coupled volume-of-fluid and level set method based on general curvilinear grids with accurate surface tension calculation," *Journal of Computational Physics*, Vol. 396, 2019, pp. 799–818.

[18] Thorpe, S. A., "Experiments on the instability of stratified shear flows: immiscible fluids," *Journal of Fluid Mechanics*, Vol. 39, No. 1, 1969, pp. 25–48.

[19] Aphale, S. S., Budzinski, K., Surina, G., and DesJardin, P. E., "Influence of O_2 Concentration in Oxidizer on Soot Formation and Radiative Heat Flux in PMMA-Air 2D Slab Burner for Understanding Hybrid Rocket Combustion," *Combustion and Flame*, (under review).

[20] Aphale, S. S., and DesJardin, P. E., "On the Role of Soot and Radiative Heat Flux for Flame Spread Along Solid Fuels," *12th U.S. National Combustion Meeting*, College Station, Texas, 2021, pp. 1–10.

[21] "Center for Computational Research, University at Buffalo," `http://hdl.handle.net/10477/79221`, 2020-2021.